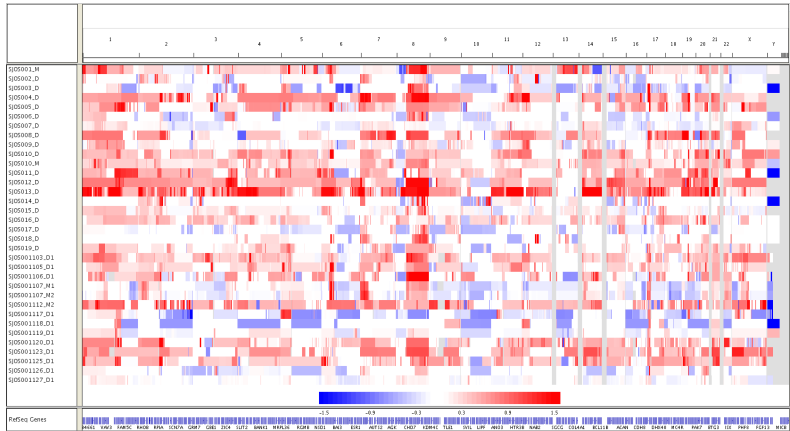
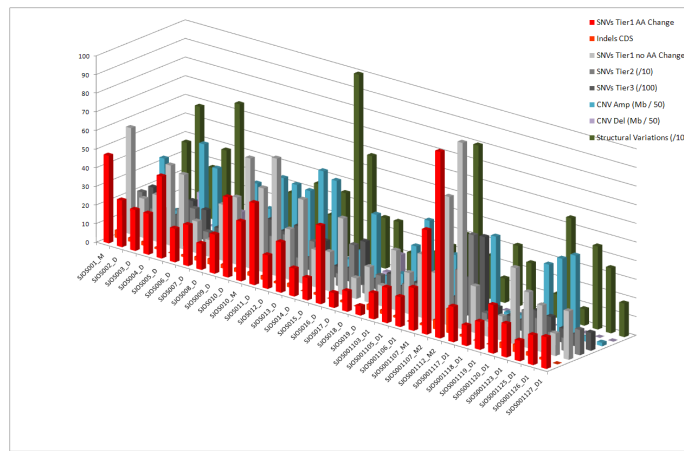


SUPPLEMENTAL DATA

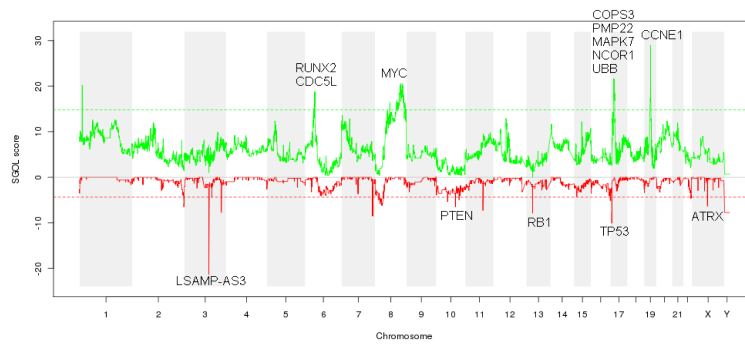
A



B

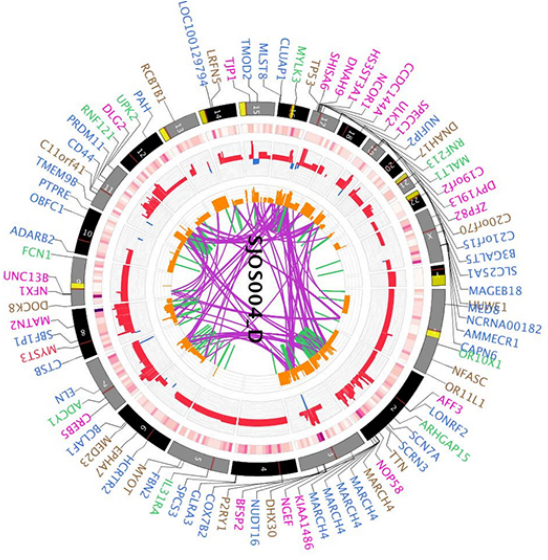


C

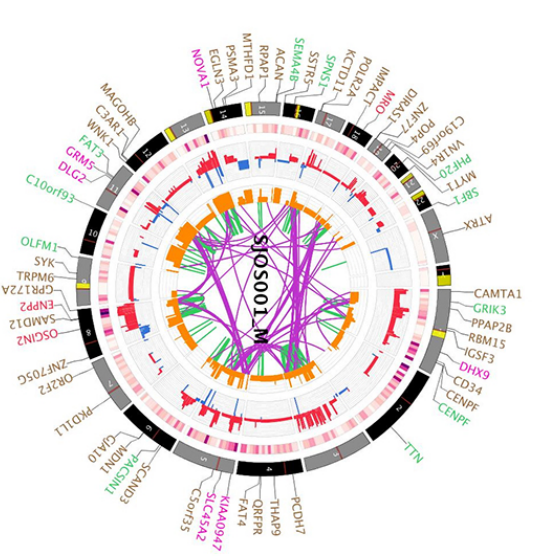


D

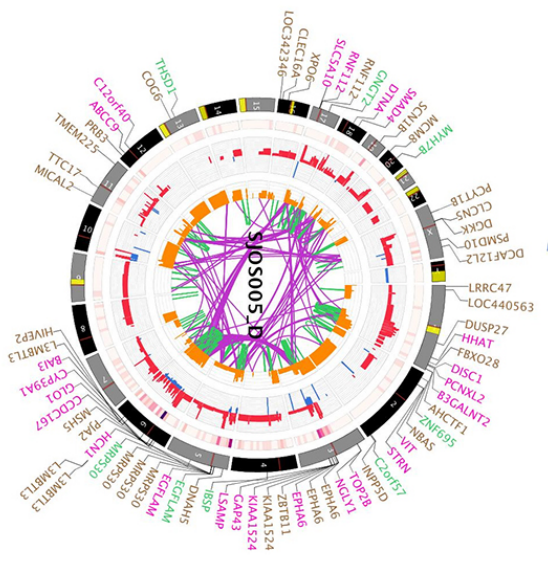
Labels for gene disrupting SVs removed



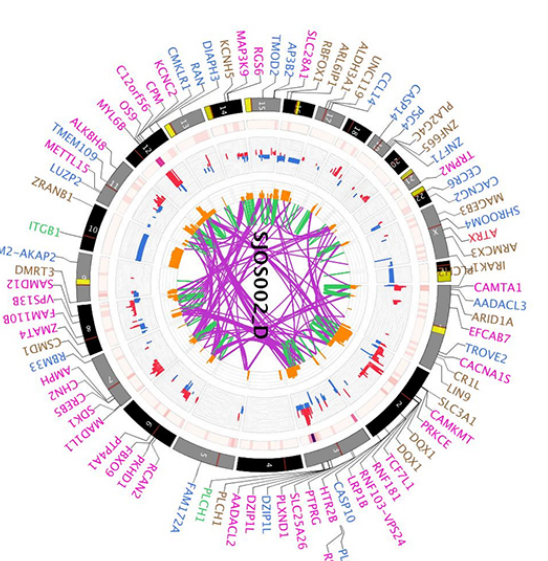
Labels for gene disrupting SVs removed



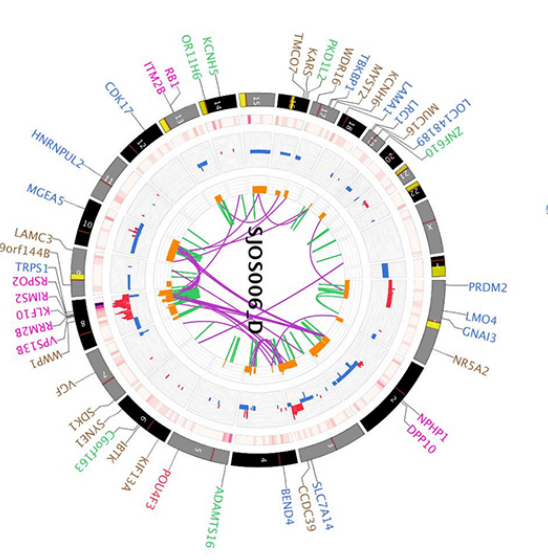
Labels for gene disrupting SVs removed

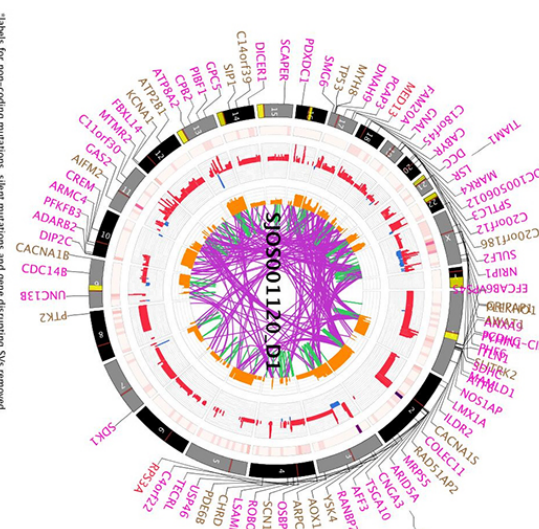
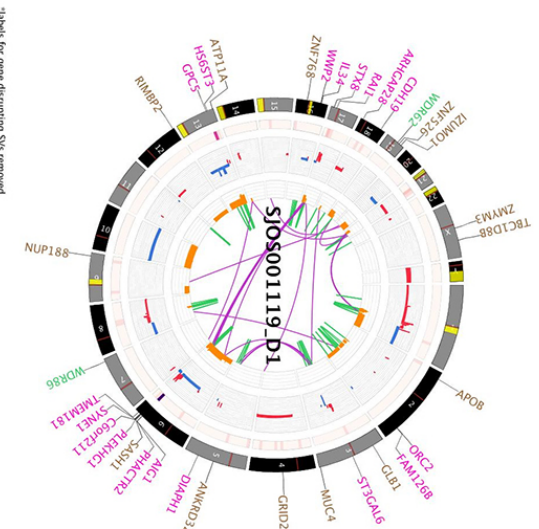
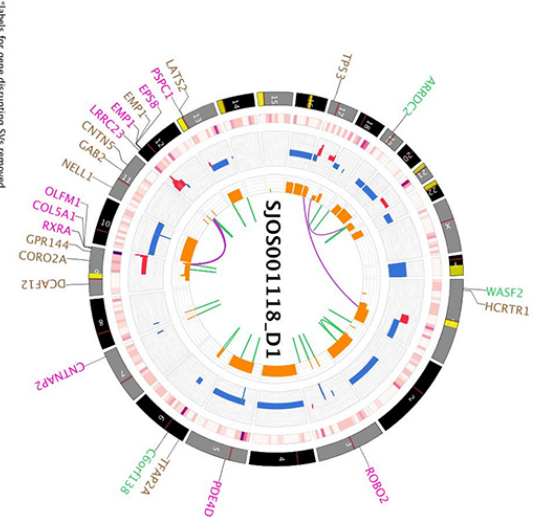
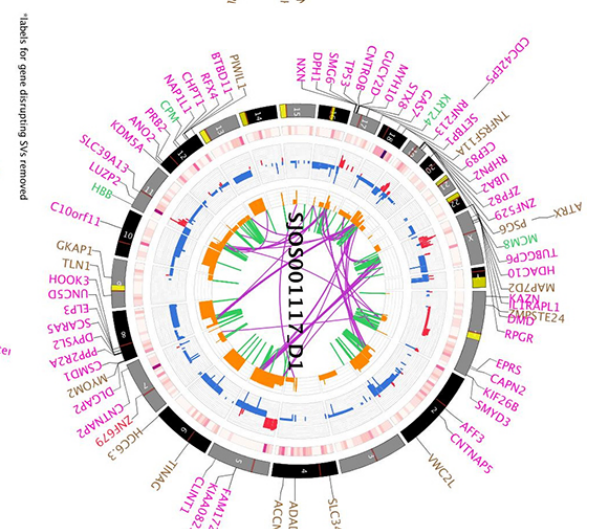
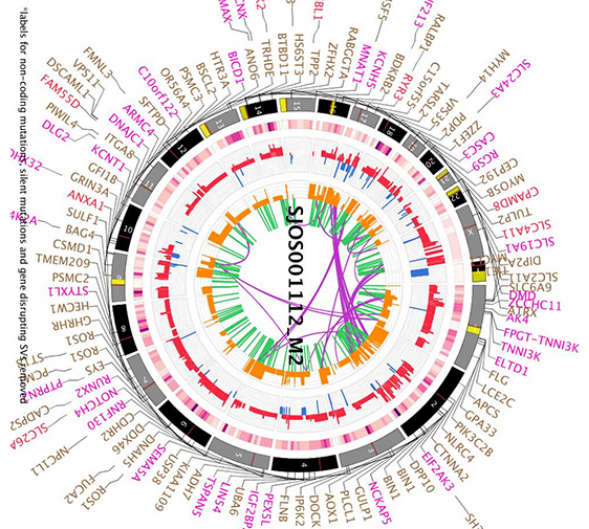
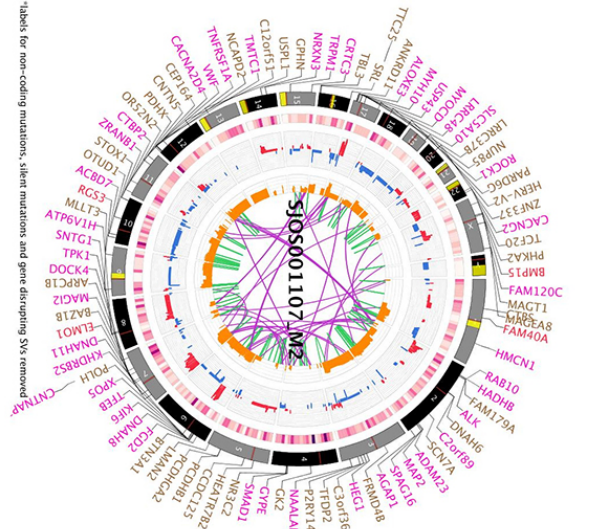


Labels for gene disrupting SVs removed



Labels for gene disrupting SVs removed

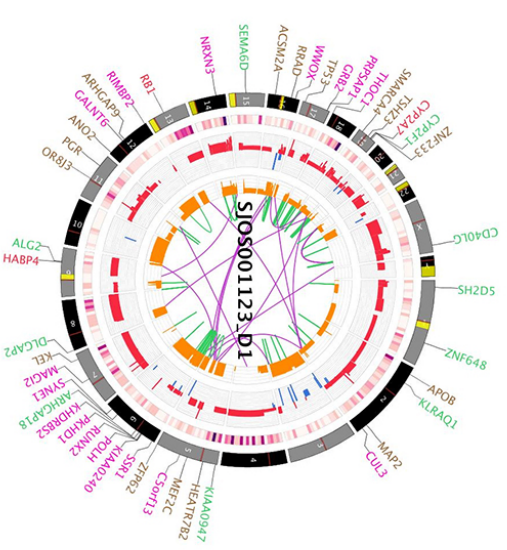




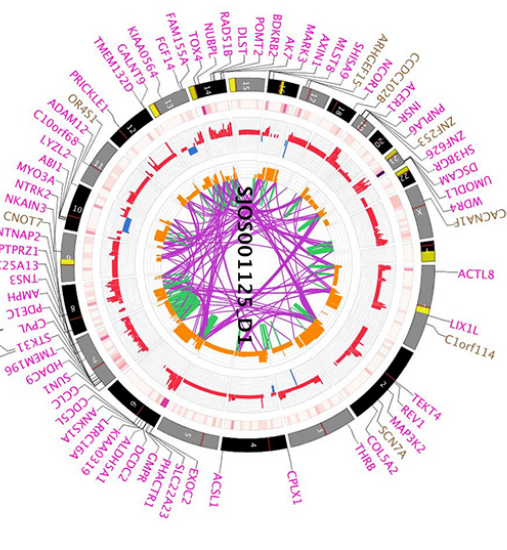
*labels for gene disrupting SVs removed

*labels for gene disrupting SVs removed

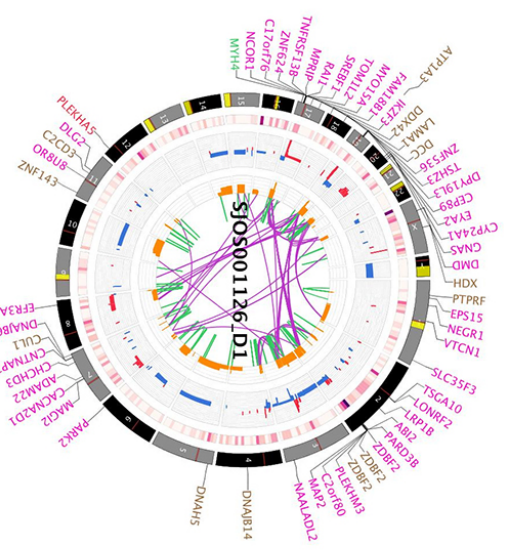
*labels for gene disrupting SVs removed



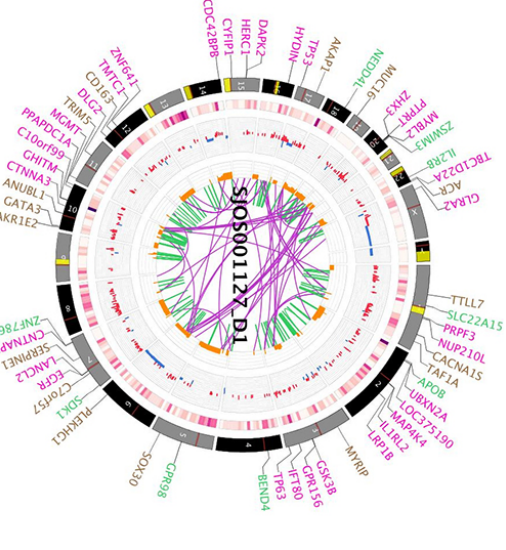
*labels for gene disrupting SVs removed



*labels for non-coding mutations, silent mutations and gene disrupting SVs removed



*labels for gene disrupting SVs removed



*labels for gene disrupting SVs removed

Figure S1 related to Figure 1. Copy number analysis of osteosarcoma discovery cohort. **A)** Copy number analysis for all 34 osteosarcomas in the discovery cohort with red indicating gain and blue indicating loss. **B)** Histogram of the type of mutations (SNV, CNV, SV, indel) across the osteosarcoma tumors in the discovery cohort. **C)** GISTIC analysis of the copy number changes in the osteosarcoma discovery cohort with green indicating gains and red indicating loss. The dashed lines represent cutoff for statistical significance and the individual chromosomes are labeled along the bottom of the plot. **D)** CIRCOS plots of all 34 tumors sequenced by WGS in this study.

Table S1 related to Figure 1. Clinical features of discovery and validation cohorts.

Provided as a separate file.

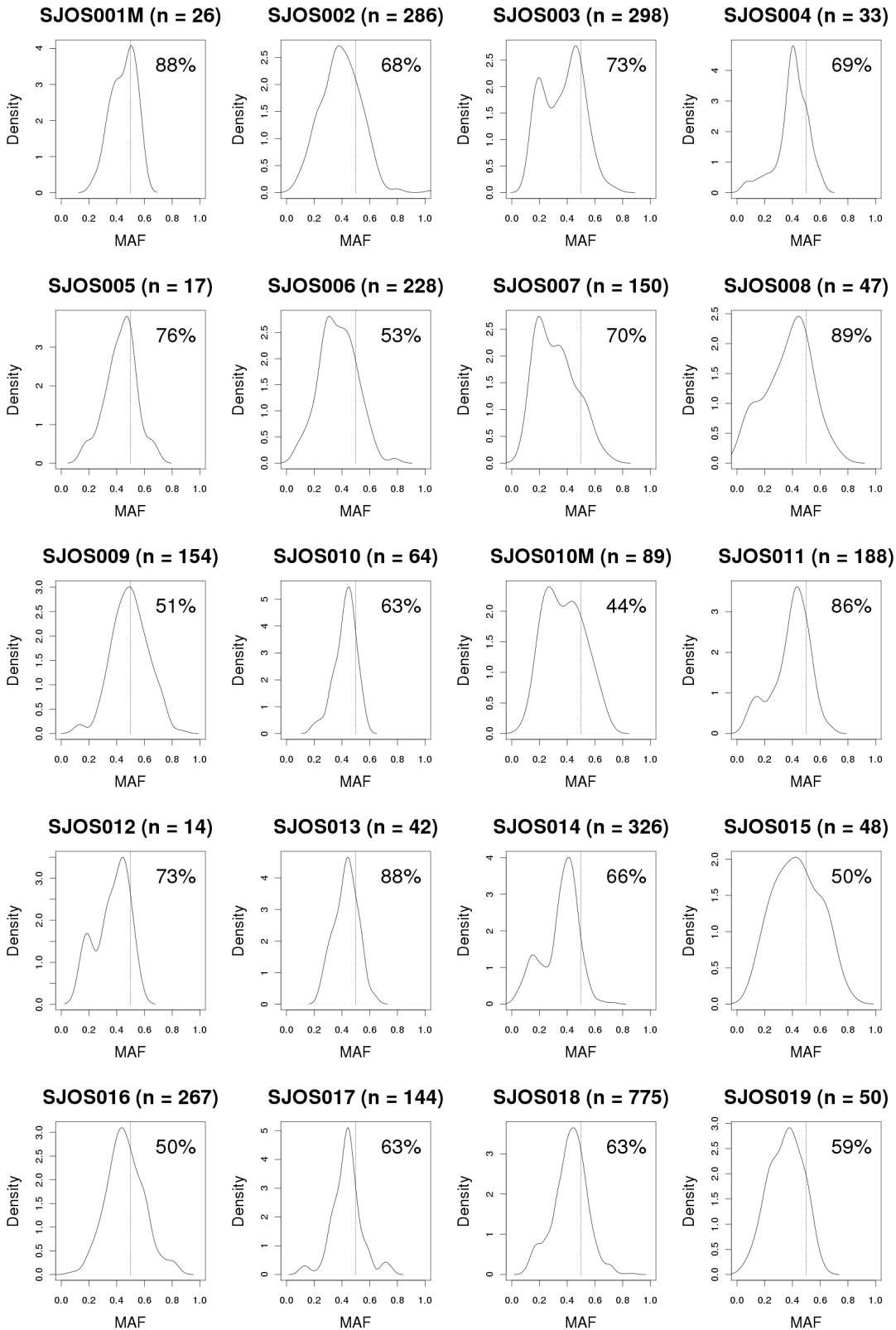
Table S2 related to Figure 1. Sequence coverage data.

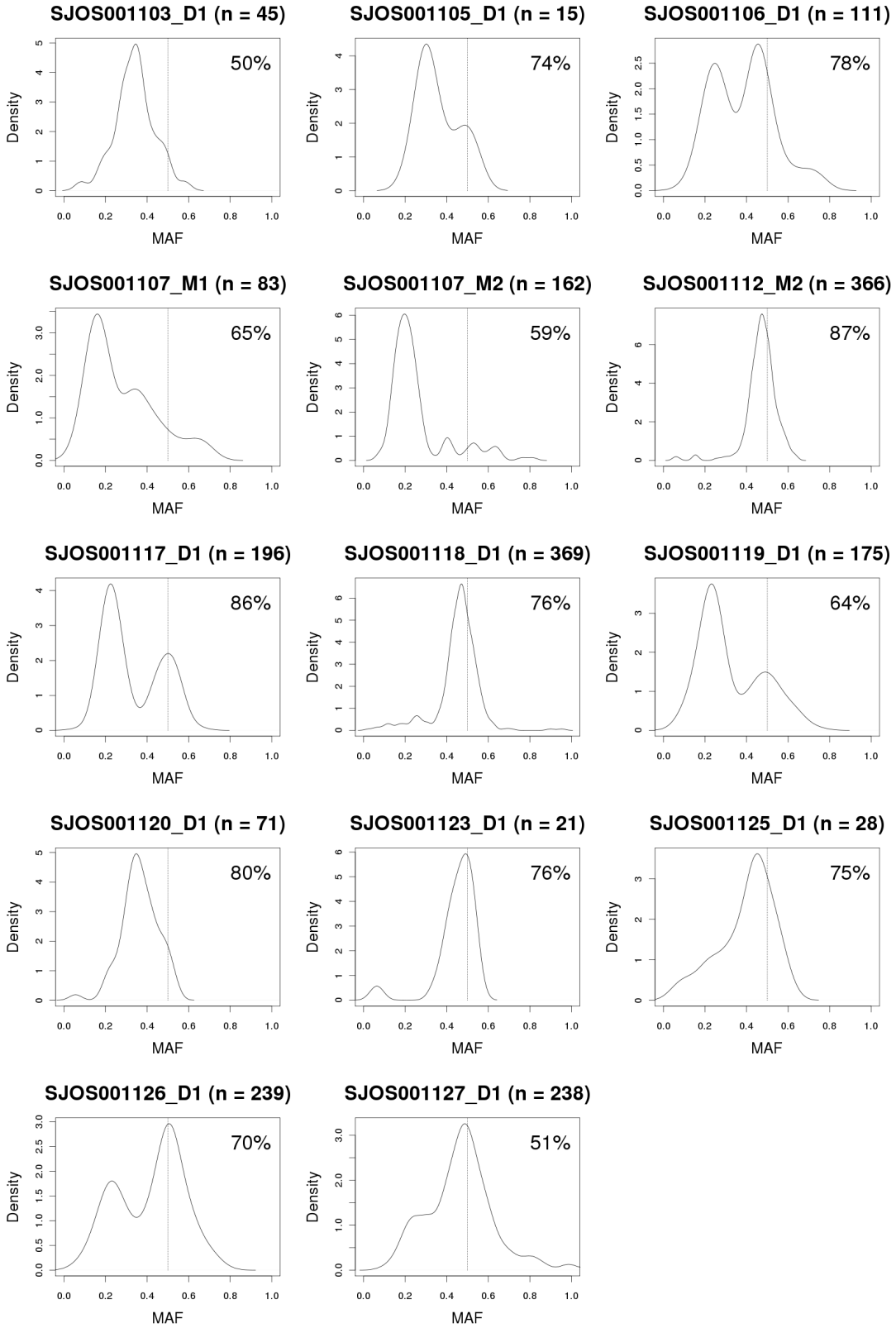
Provided as a separate file.

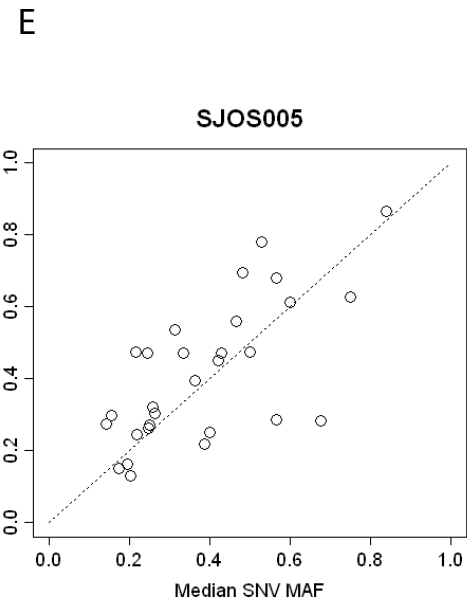
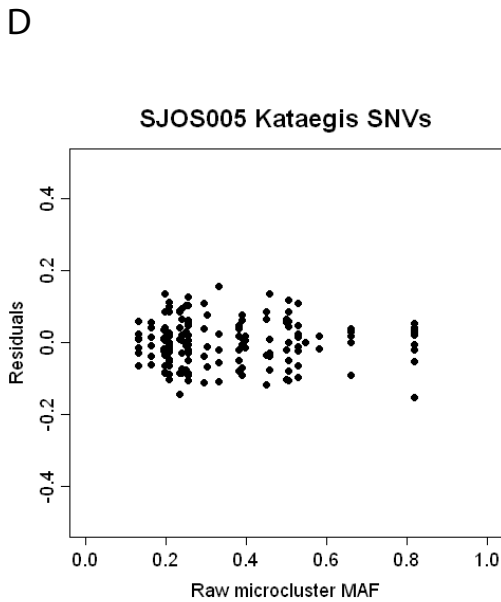
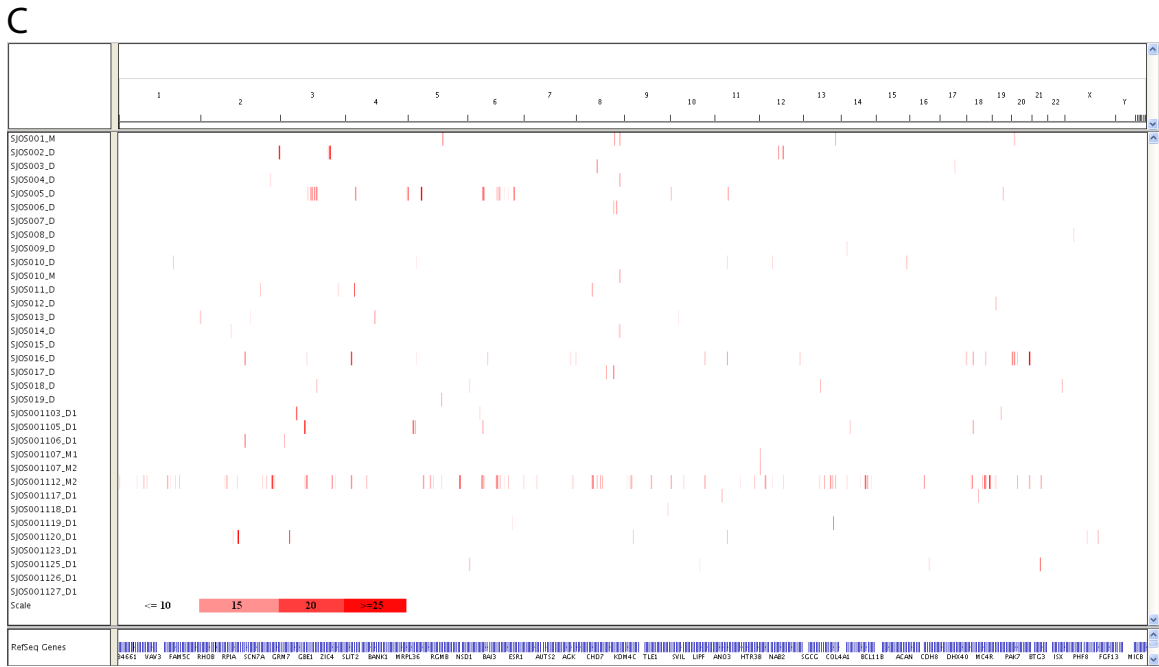
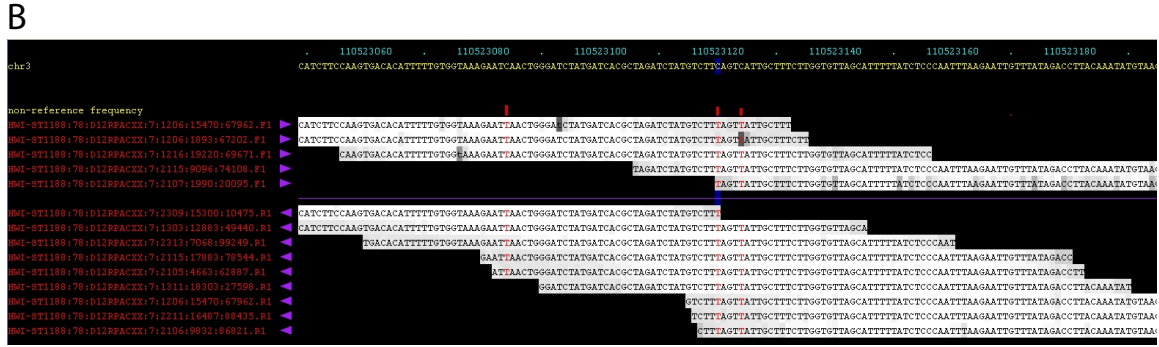
Table S3 related to Figure 1. Validated mutations.

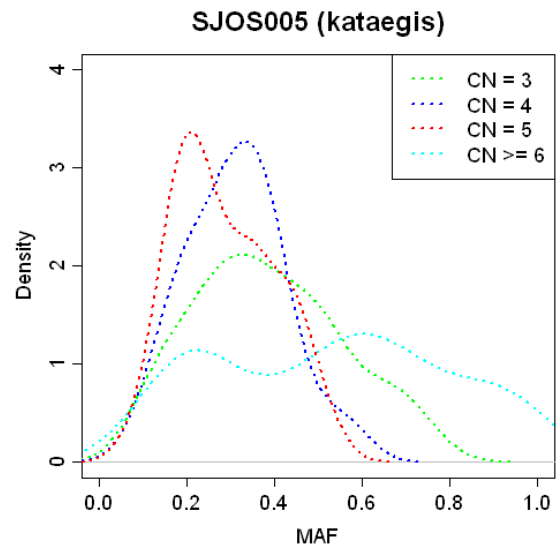
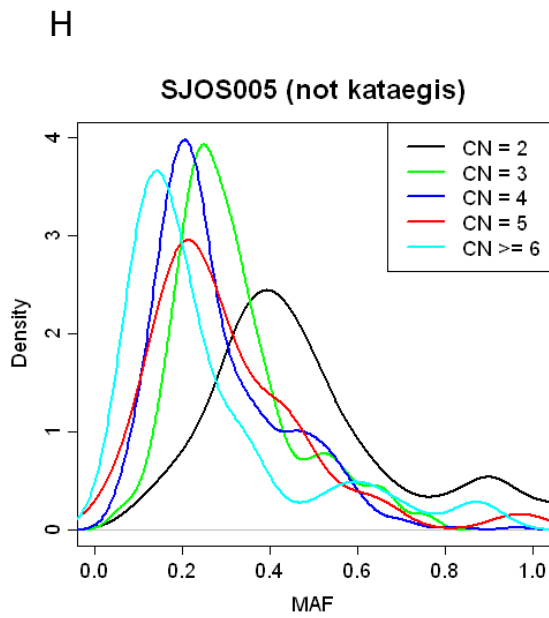
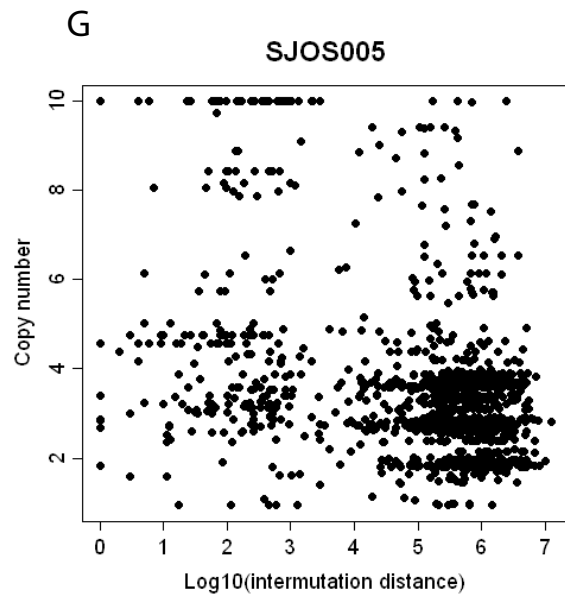
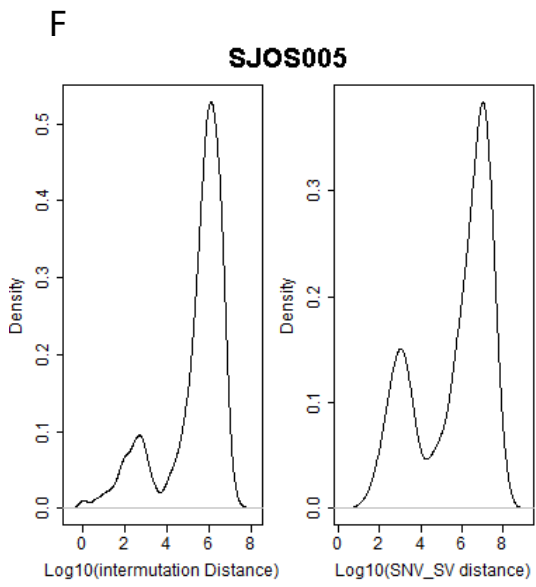
Provided as a separate file.

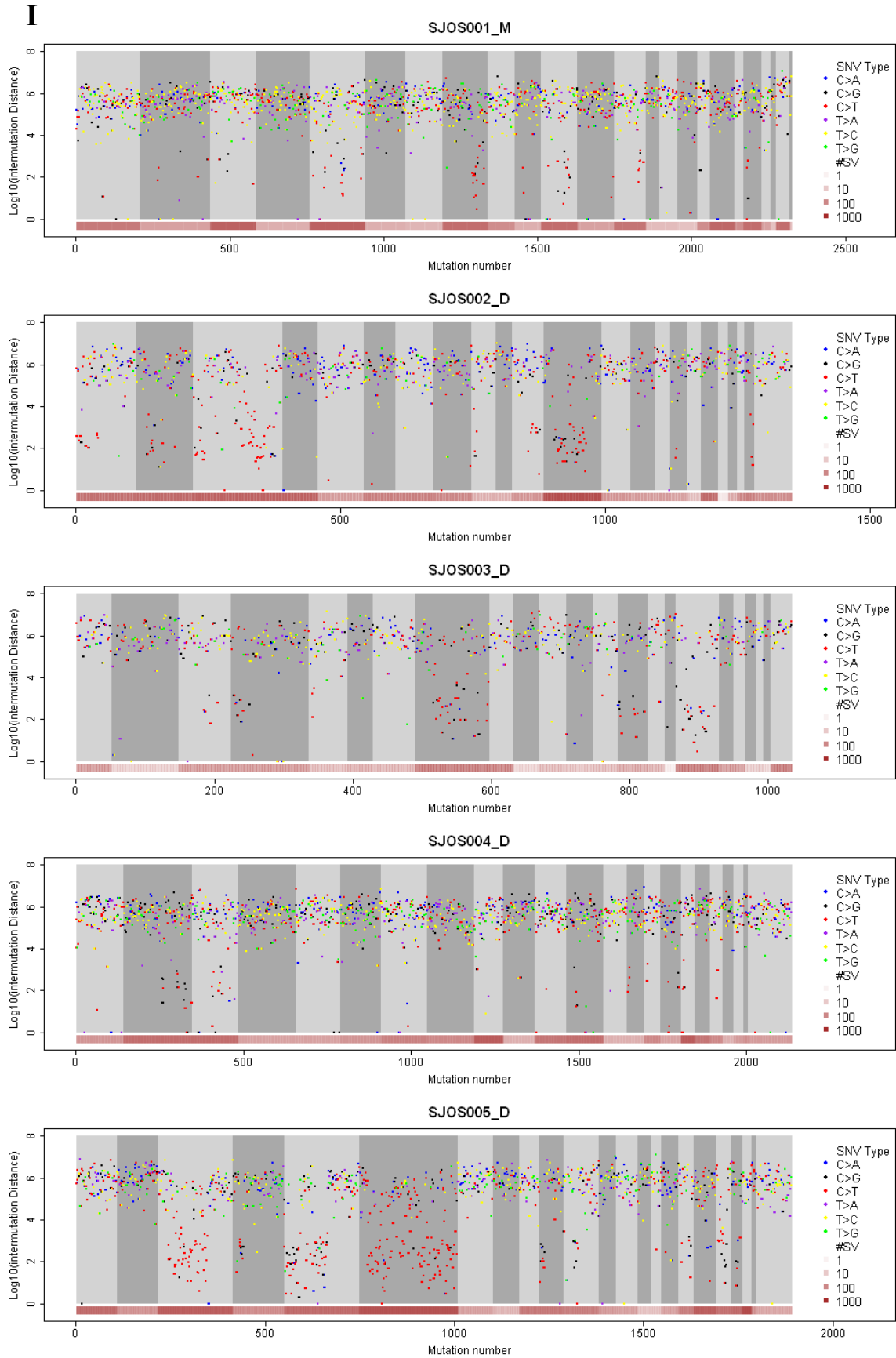
A

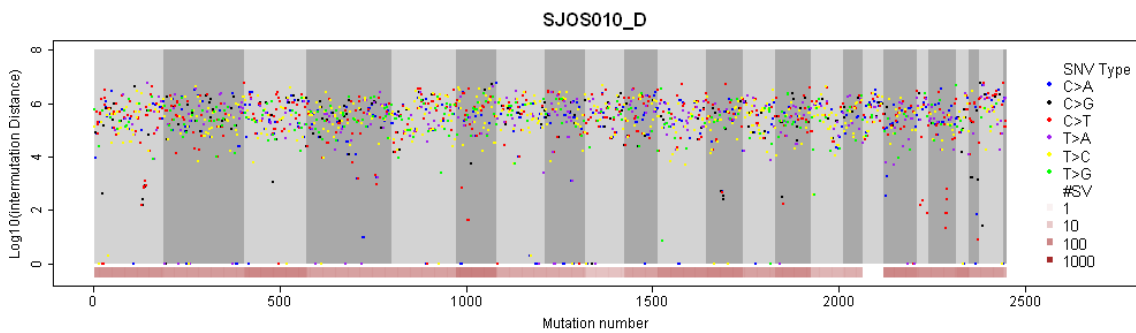
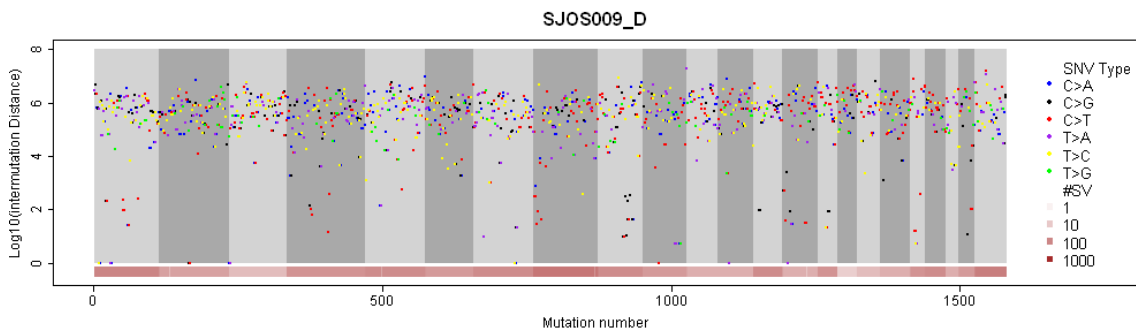
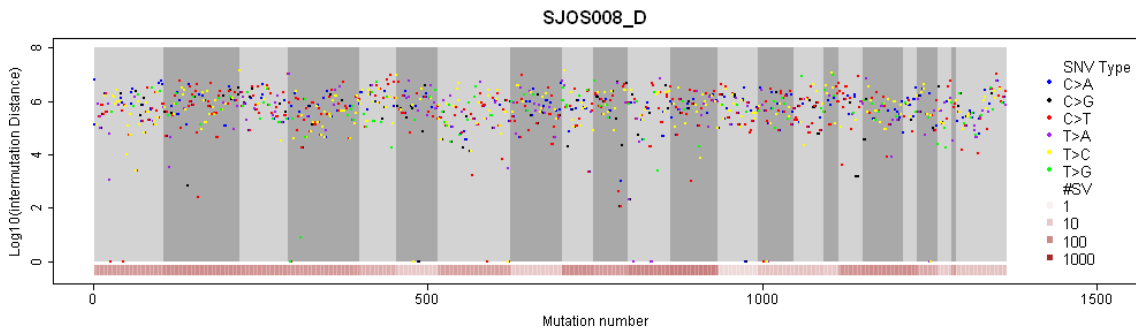
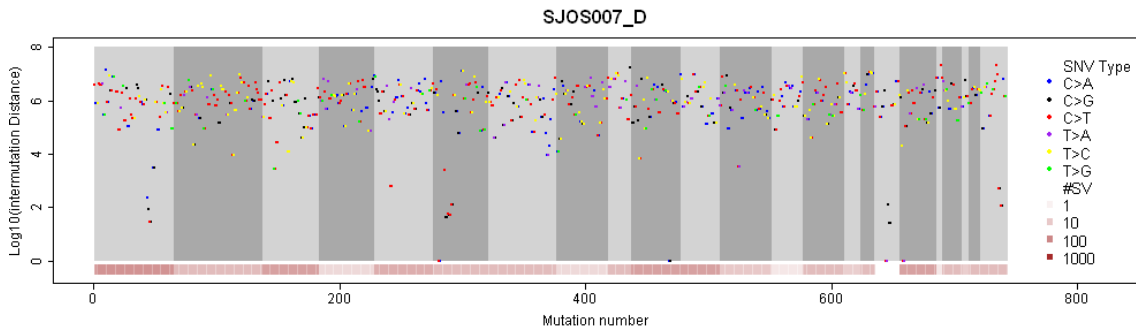
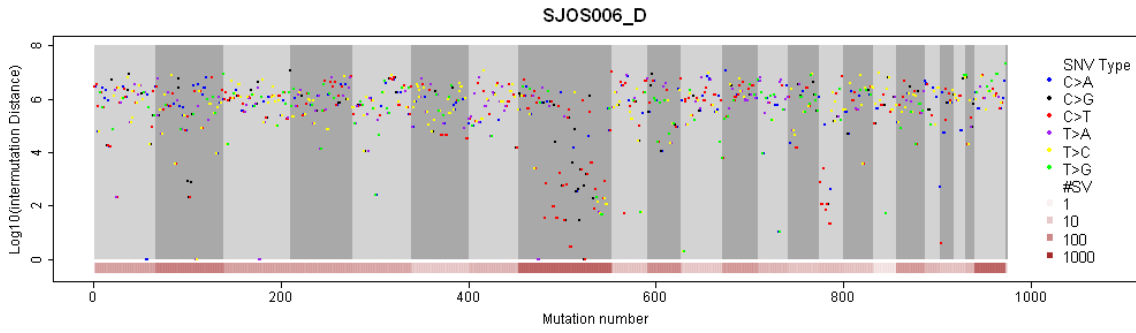


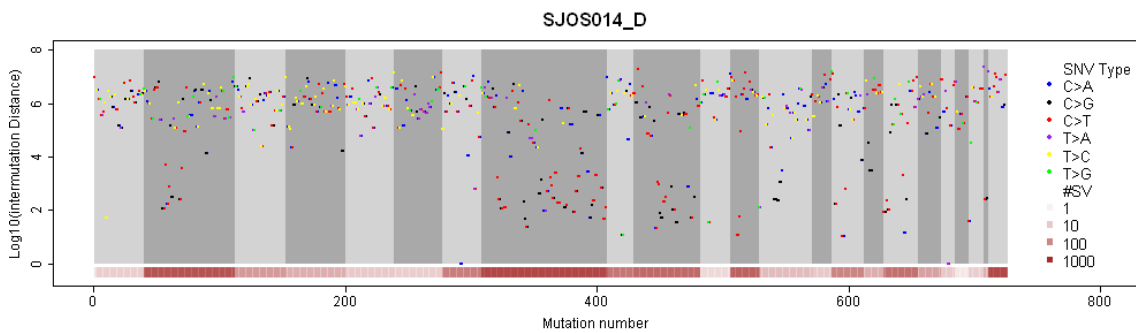
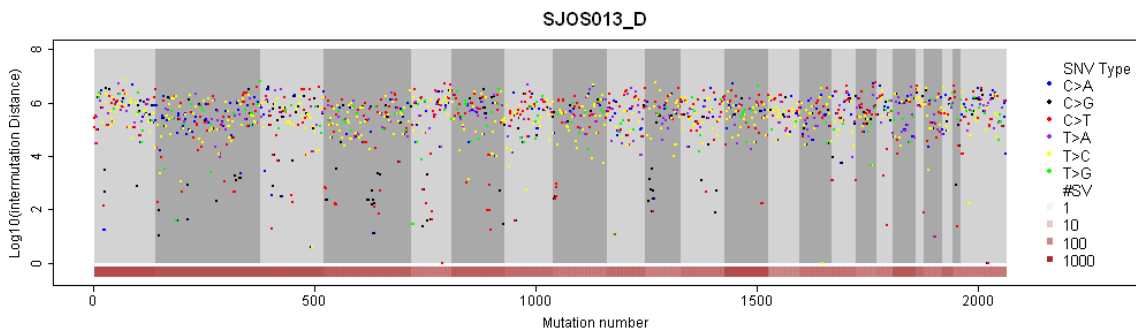
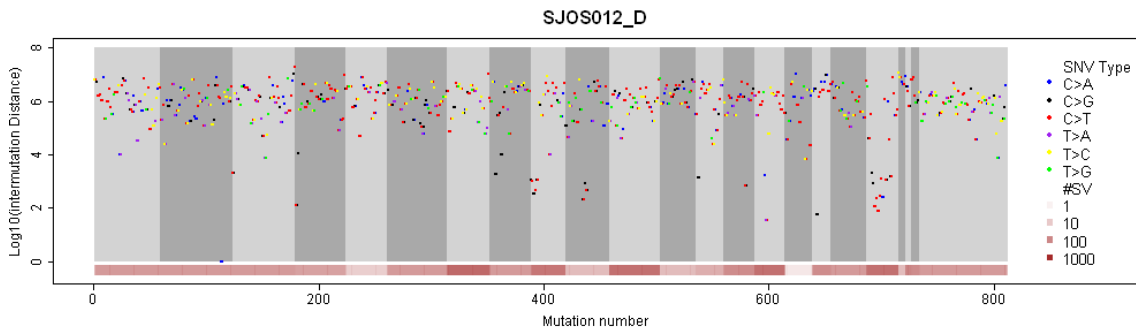
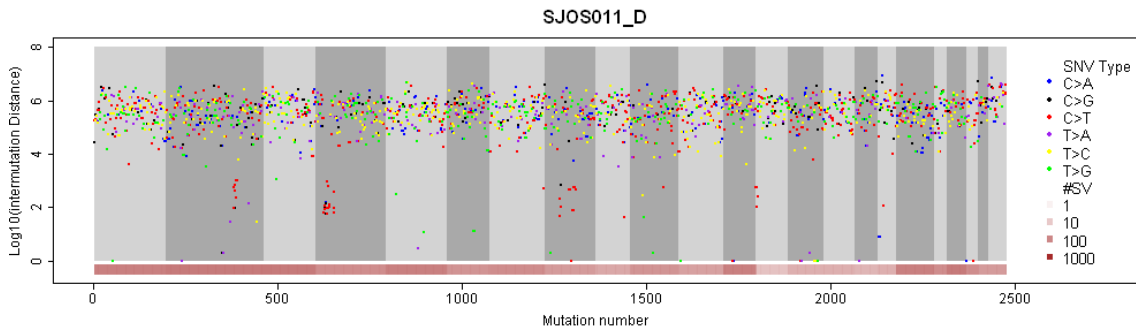
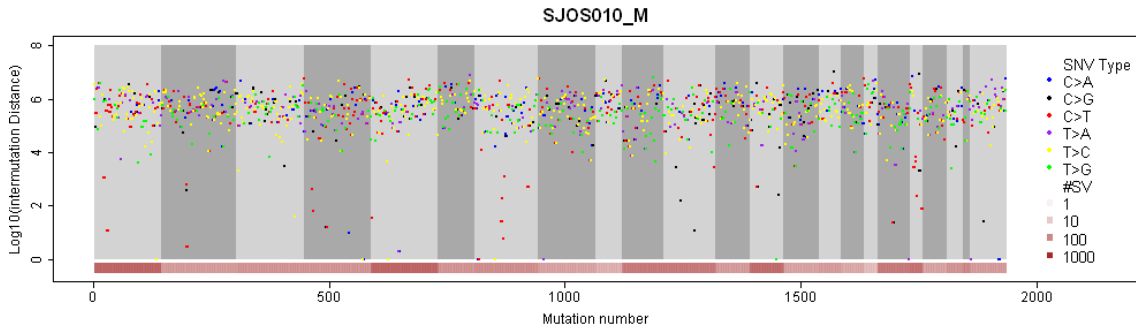


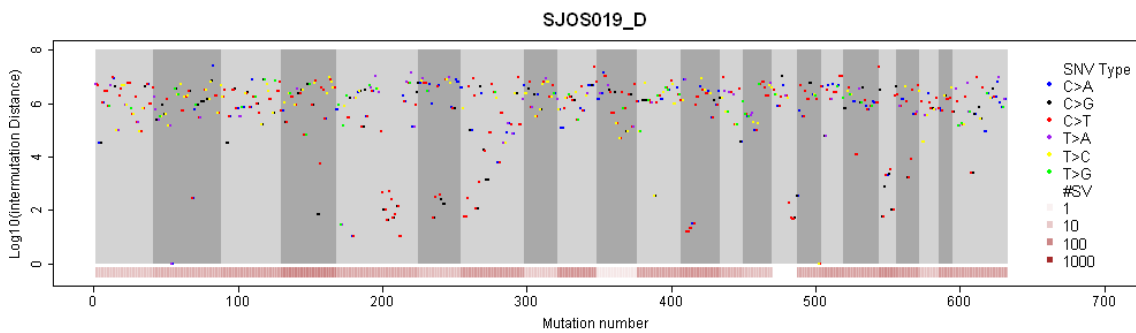
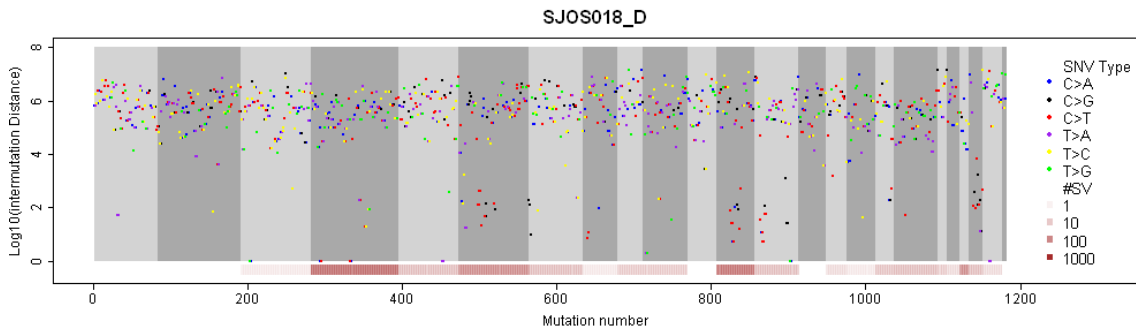
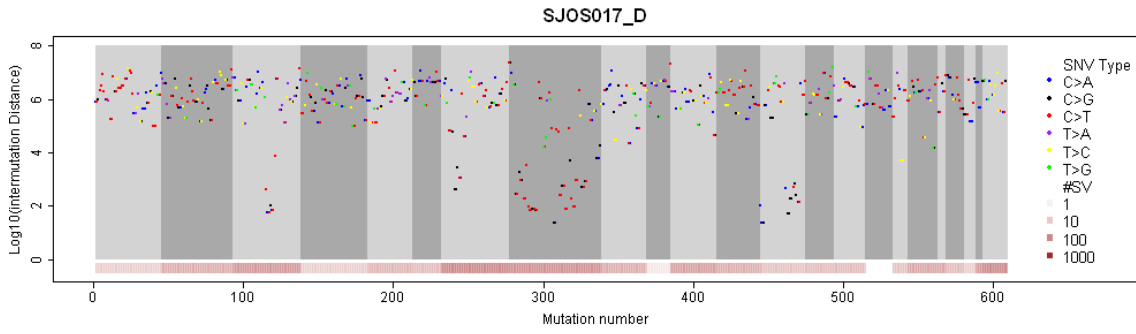
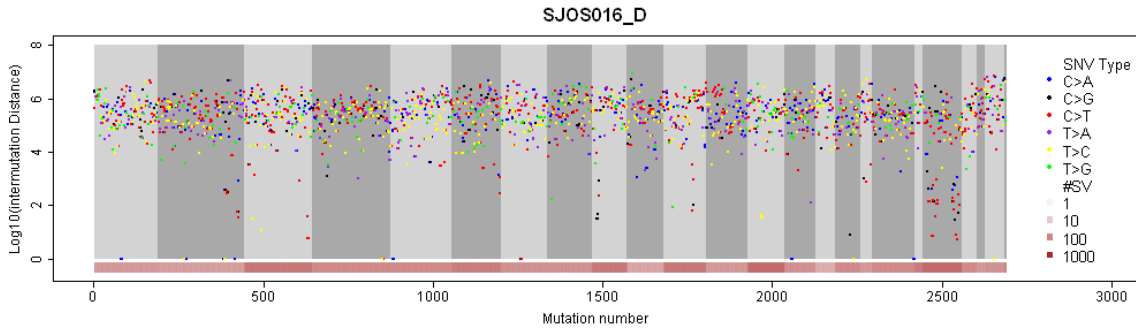
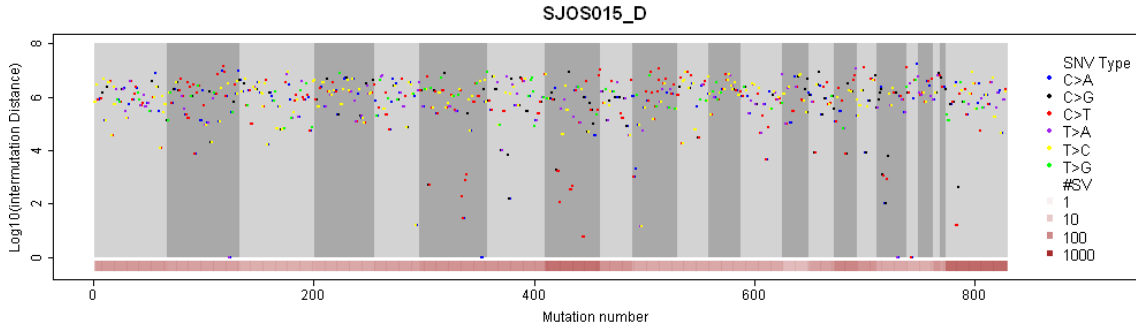


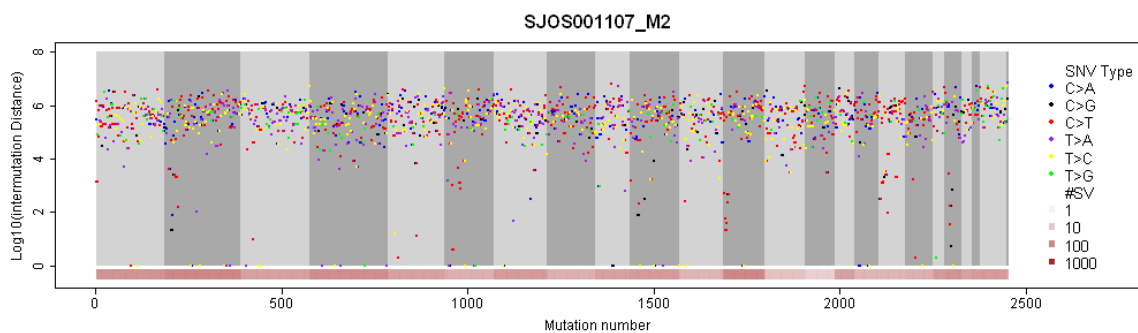
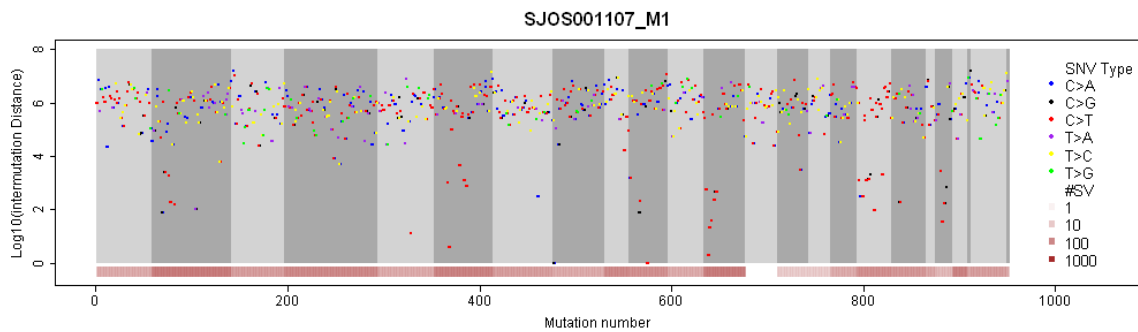
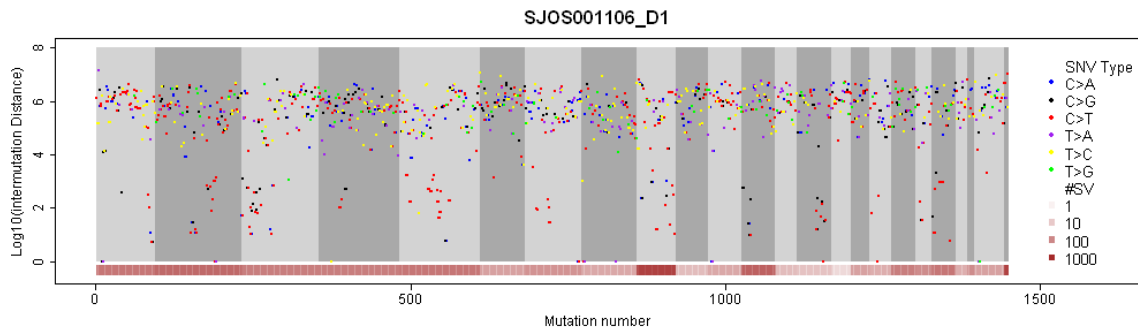
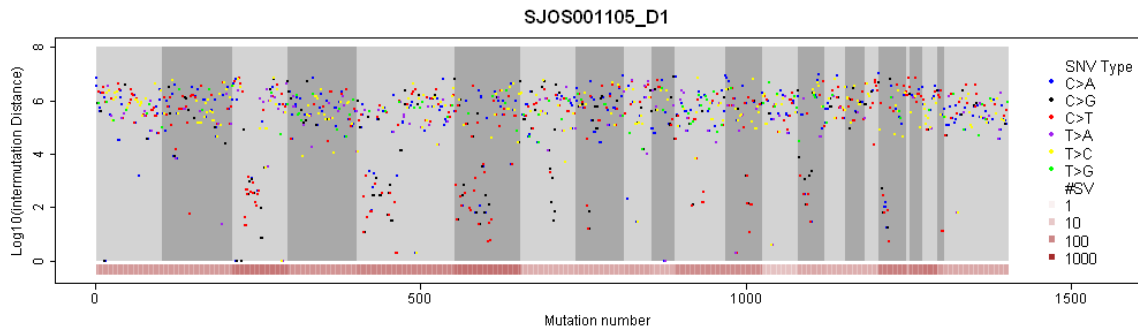
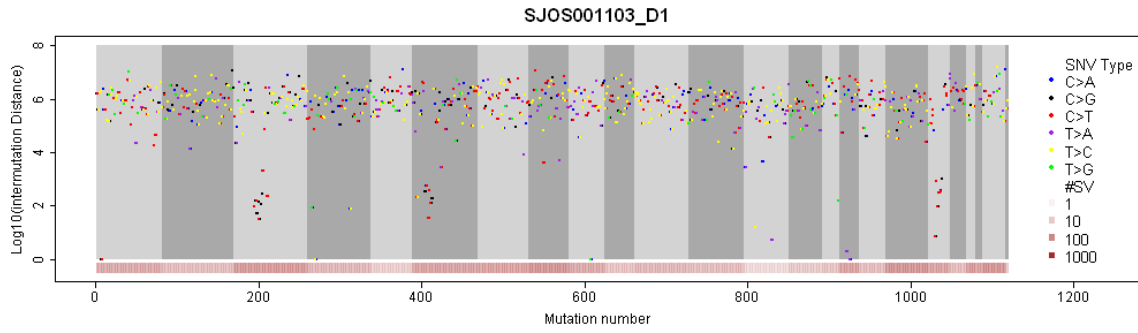


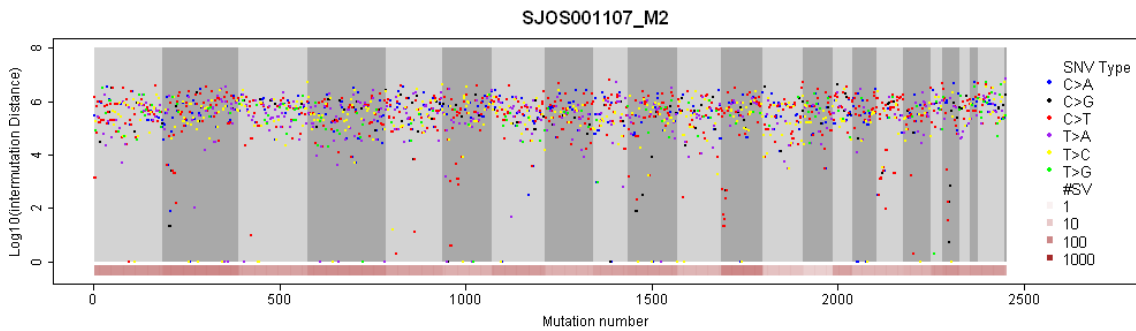
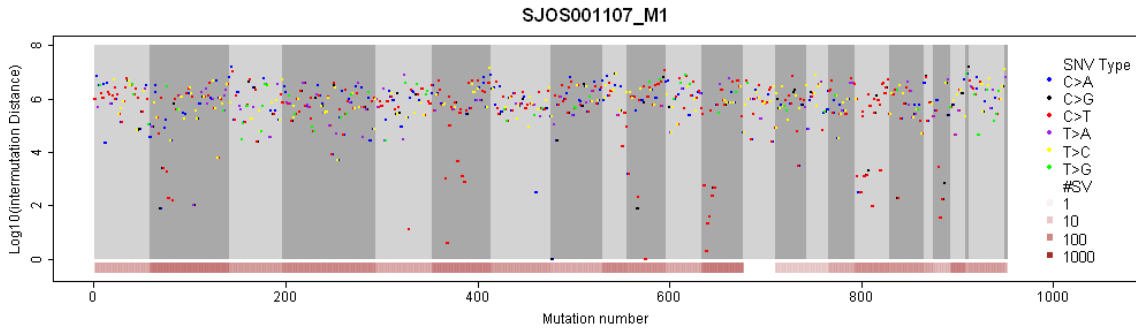
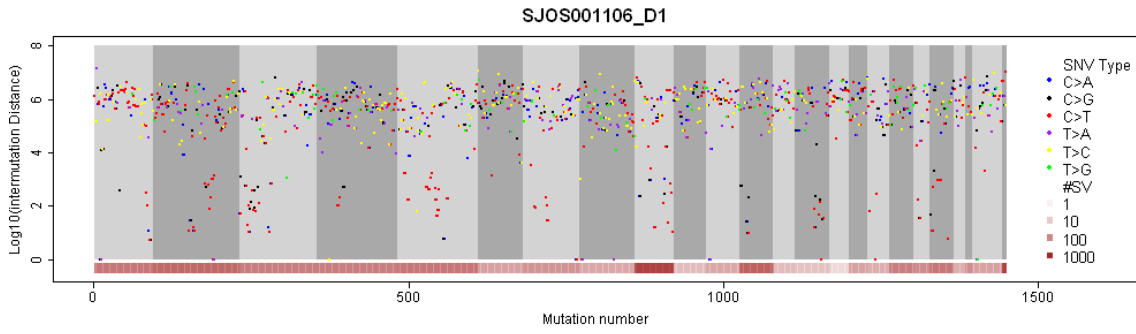
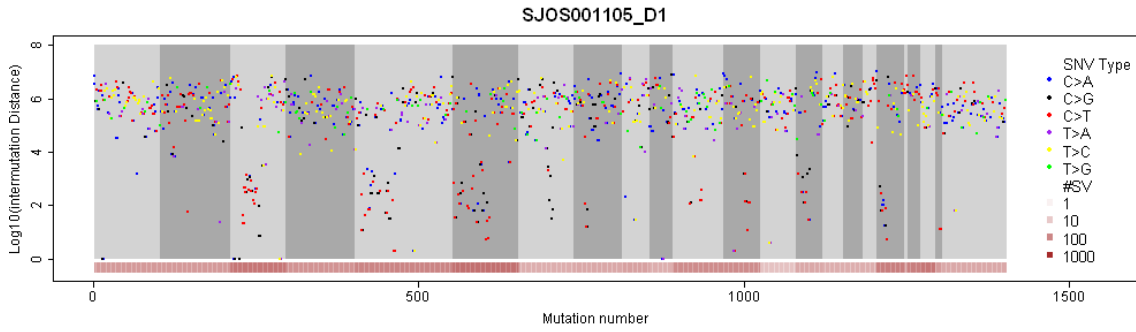
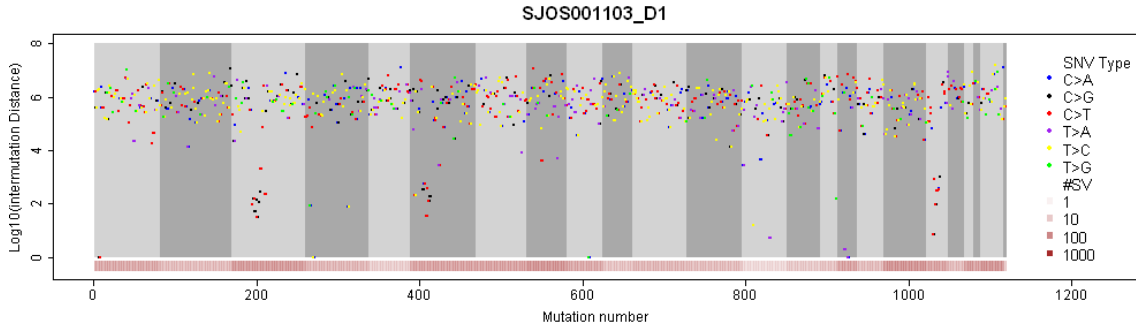


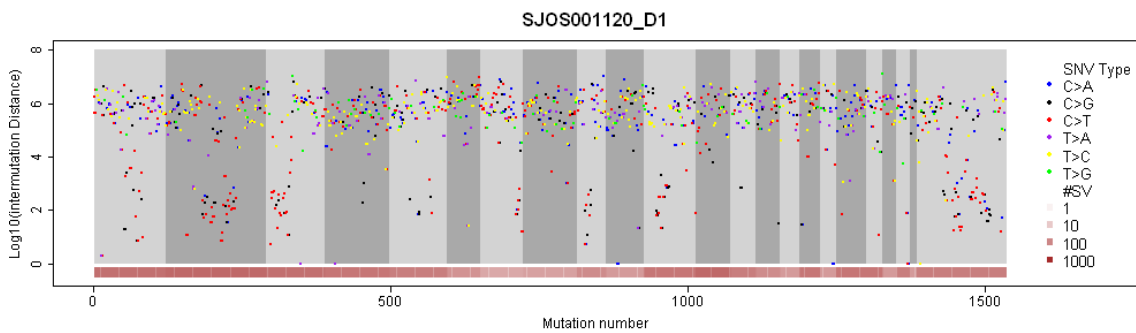
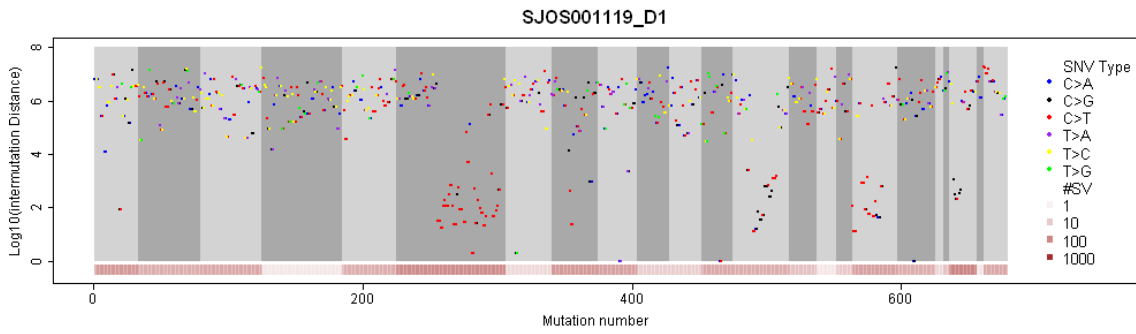
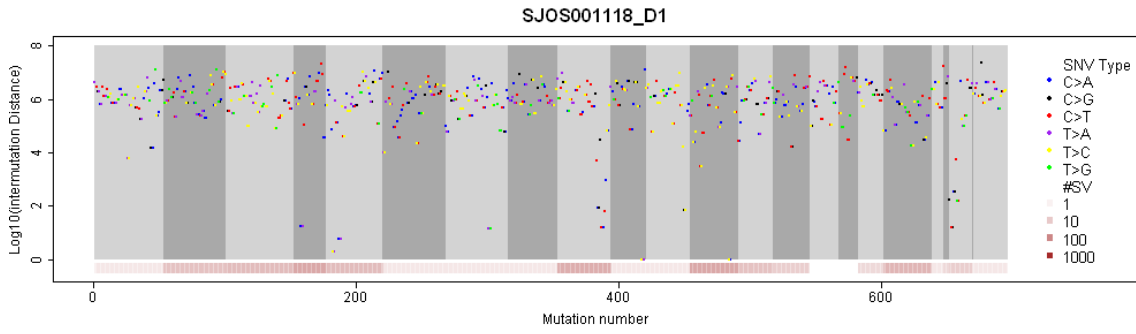
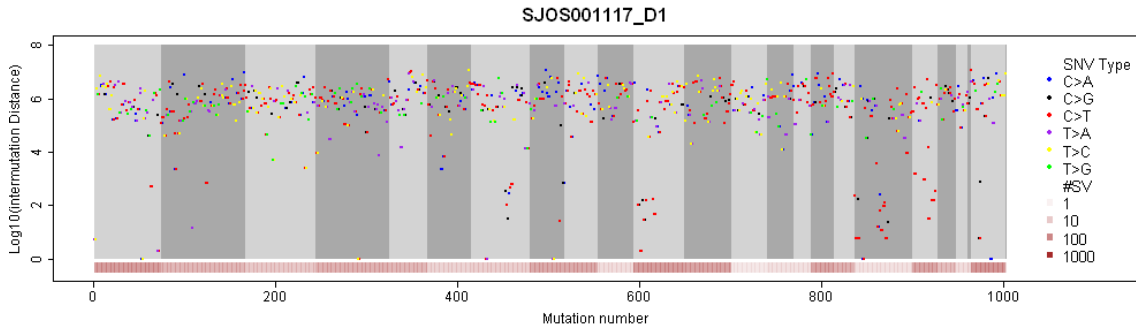
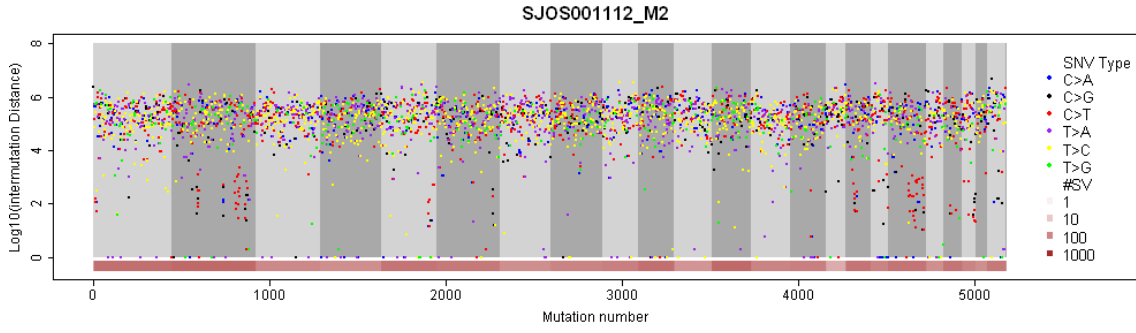












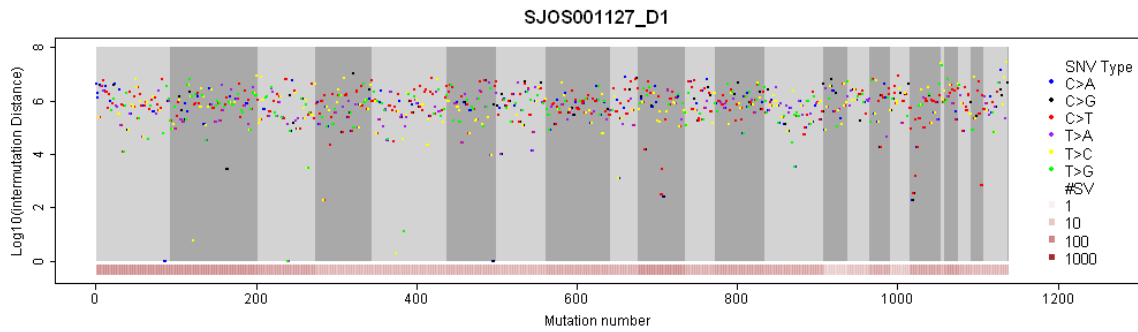
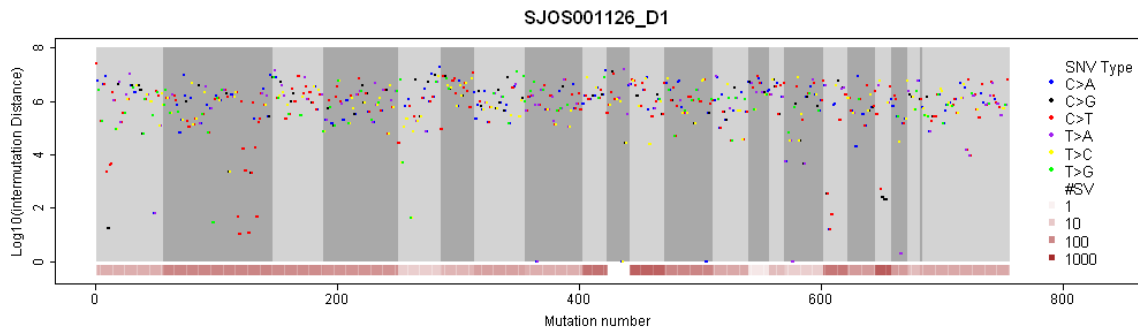
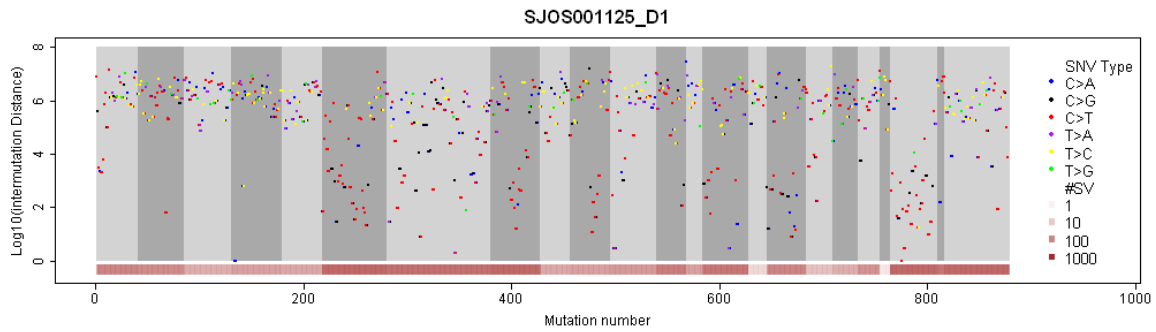
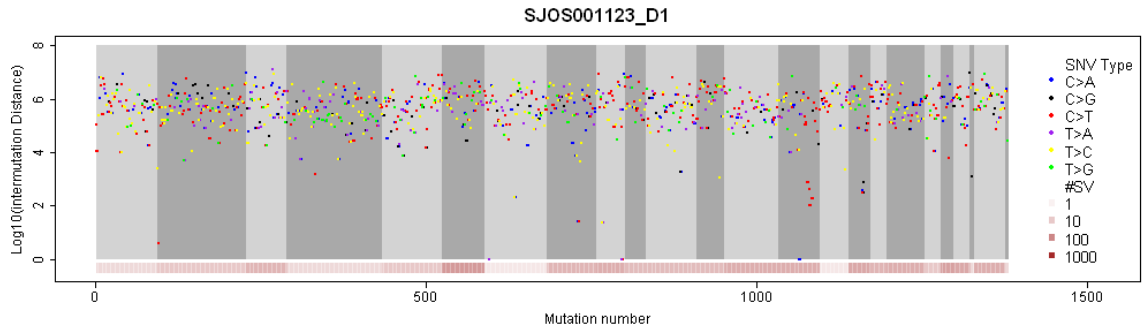
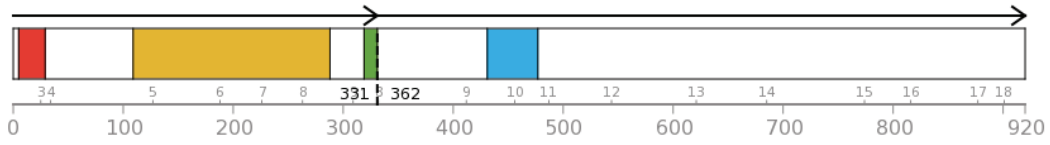


Figure S2 related to Figure 2. Analysis of tumor heterogeneity and kataegis. A) Tumor purity adjusted mutant allele fraction (MAF) for samples analyzed by whole genome sequencing. The actual tumor purity that was used to adjust the MAF is shown as a percentage for each tumor. The number of qualifying SNVs (n) used to plot the density plot is shown for each tumor. **B)** Screenshot of WGS data with individual sequence reads showing kataegis hypermutation on the same DNA strand. **C)** Genomewide distribution of mutation hotspots in osteosarcoma shown as the ratio between observed mutation rate in the window over the genomewide mutation rate within a 3.2 Mb window across the genome for the 34 samples analyzed by WGS. **D)** Kataegis SNVs showed different MAFs among different microclusters although SNVs within a microcluster shared similar MAFs. **E)** Comparison of MAFs of SVs and SNVs in kataegis regions. **F)** The distribution of intermutation distance and distance from a SNV to nearest SV breakpoint in SJOS005, showing majority of mutations in the genome have a intermutation distance around 1 Mb while a small portion of SNVs have an intermutation distance smaller than 10 kb. **G)** Distribution of copy number variation and SNV intermutation distance (log10) which shows higher proportion of closely spaced SNVs (i.e. kataegis SNVs) occur in amplified regions. **H)** Distribution of mutant allele fraction of non-kataegis SNVs (left panel) and kataegis SNVs (right panel) in regions of different copy number state in SJOS005. SNVs acquired before amplification show multiple mutant allele fraction (MAF) peaks, depending on whether the mutant allele or the reference allele is amplified while mutations acquired after amplification showed a single MAF corresponding to mutation on a single copy. **I)** Rainfall plot of all 34 genomes in the WGS cohort.

A



TP53-SFSWAP

NM_000546-NM_004592

- P53_TAD - P53 transactivation motif...
- P53 - P53 DNA-binding domain...
- P53_tetramer - P53 tetramerisation motif...
- Surp - Surp module...

B

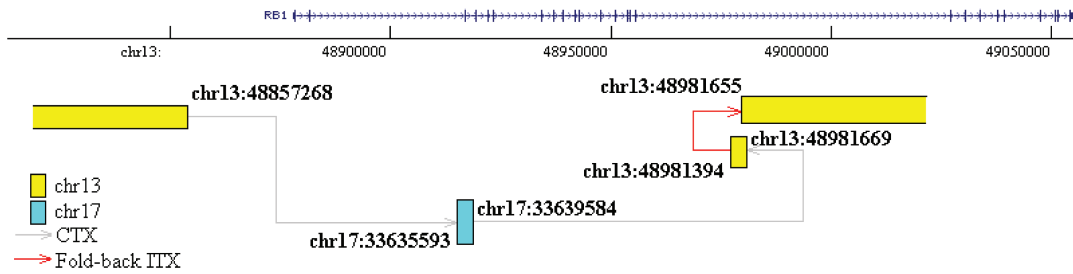
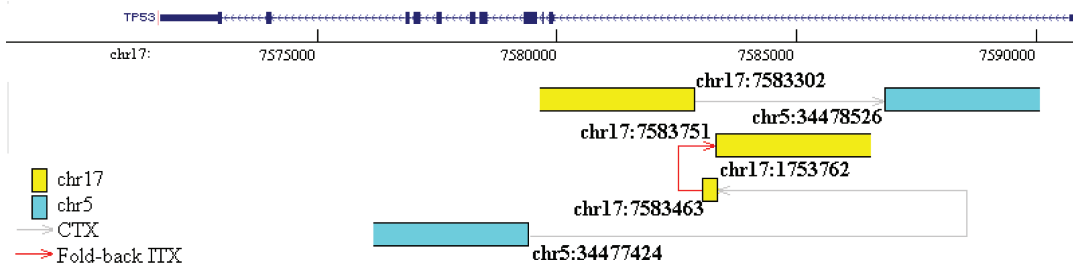


Figure S3 related to Figure 3. *TP53* translocations in osteosarcoma. A) Diagram of the predicted fusion gene generated by the interchromosomal translocation between the *TP53* gene and the *SFSWAP* gene in SJOS007_D. B) Diagram of the fold-back translocation in the *TP53* gene in SJOS001_M (upper panel). Diagram of the fold-back translocation in the *RBI* gene in SJOS015_D (lower panel). The translocations are indicated by the red arrows.

Table S4 related to Figure 3. Analysis of p53 mutations in osteosarcoma.

Provided as a separate file.

Table S5 related to Figure 4. Analysis of p53 analysis and clinical features.

Provided as a separate file.

Table S6 related to Figure 5. ATRX analysis in osteosarcoma.

Provided as a separate file.

Table S7 related to Figure 5. Cancer gene mutations in osteosarcoma.

Provided as a separate file.